

## Highest optical gap tetrahedral amorphous carbon

K.B.K. Teo<sup>a</sup>, A.C. Ferrari<sup>a,\*</sup>, G. Fanchini<sup>b</sup>, S.E. Rodil<sup>a</sup>, J. Yuan<sup>a</sup>, J.T.H. Tsai<sup>a</sup>, E. Laurenti<sup>c</sup>,  
A. Tagliaferro<sup>b</sup>, J. Robertson<sup>a</sup>, W.I. Milne<sup>a</sup>

<sup>a</sup>Engineering Department, University of Cambridge, Cambridge CB2 1PZ, UK

<sup>b</sup>Physics Department and INFN Unit, Politecnico di Torino, Torino, Italy

<sup>c</sup>Chemistry Department I.F.M., Università di Torino, Torino, Italy

### Abstract

The deposition and characterisation of tetrahedral amorphous carbon (ta-C) with an  $E_{04}$  optical gap of 3.5 eV and Tauc gap of 3 eV is presented. This is the highest optical gap reported in literature for ta-C and was directly measured using photothermal deflection spectroscopy (PDS) and UV-Vis spectrophotometry. Independent PDS, UV-Vis and electron energy loss spectroscopy (EELS) measurements confirmed the high gap. A large Urbach slope of 600 meV was measured, which indicated that there are many tail states. Electron spin resonance (ESR) measurements confirmed that this material has a high spin density of  $7.5 \times 10^{20}$  spins/cm<sup>3</sup>. Post-deposition vacuum annealing of the samples to 500 °C resulted in a small increase of the optical gap,  $E_{04} \sim 3.6$  eV, and a decrease of the defects to  $2.7 \times 10^{20}$  spins/cm<sup>3</sup>. Post-deposition annealing at this temperature did not significantly change the sp<sup>3</sup> fraction, but caused a 2–3 order of magnitude increase of the conductivity and a significant reduction of the stress. Thus, this is the first demonstration that we can engineer the defects in ta-C by increasing the electron delocalisation whilst maintaining the high sp<sup>3</sup> and optical gap of the material. © 2002 Elsevier Science B.V. All rights reserved.

**Keywords:** Diamond-like carbon; Optical properties; Electron spin resonance; Defects

### 1. Introduction

The great versatility of carbon materials arises from the strong dependence of their properties on the ratio of sp<sup>2</sup> (graphite-like) to sp<sup>3</sup> (diamond-like) bonds in the material. An amorphous carbon with a high fraction of sp<sup>3</sup> bonds is named diamond-like carbon (DLC). There are many forms of sp<sup>2</sup> bonded carbons with various degrees of graphitic ordering, ranging from microcrystalline graphite to glassy carbon. In general, an amorphous carbon can have any mixture of sp<sup>3</sup>, sp<sup>2</sup> and even sp<sup>1</sup> sites, with the possible presence of up to 60 at.% hydrogen [1–3]. The hydrogenated amorphous carbons (a-C:H) have a rather small C–C sp<sup>3</sup> content. DLCs with higher sp<sup>3</sup> contents are termed tetrahedral amorphous carbon (ta-C) and their hydrogenated analogue, ta-C:H. Ta-C can be grown by a number of deposition techniques involving energetic ions or plasma beams, such as filtered cathodic vacuum arc (FCVA) [4], mass selected ion beam (MSIB) [5] and pulsed laser deposi-

tion (PLD) [6]. During the deposition process, energetic carbon ions subplant in the growing film to form dense and metastable sp<sup>3</sup> bonding [4,5].

The basic electronic structure of amorphous carbon consists of strong  $\sigma$  bonds of sp<sup>3</sup> and sp<sup>2</sup> sites forming the occupied bonding ( $\sigma$ ) states in the valence band and the empty antibonding ( $\sigma^*$ ) states in the conduction band, separated by a wide gap of  $\sim 5$  eV [1–3]. The  $\pi$  bonds of sp<sup>2</sup> and sp<sup>1</sup> sites give rise to occupied  $\pi$  and unoccupied  $\pi^*$  states which lie largely within the  $\sigma$ – $\sigma^*$  gap and thus control the effective gap of the material. Diamond has a band gap of 5.5 eV, room temperature conductivity of  $10^{-18}$   $\Omega$  cm<sup>-1</sup>, density of 3.515 g/cm<sup>3</sup> and an isotropic average Young's modulus of 1144.6 GPa. It has been possible to deposit uniform ta-C films with 88% sp<sup>3</sup>, 3.3 g/cm<sup>3</sup> density [7] and 760 GPa Young's modulus [8], which directly correlate with the mechanical properties of diamond when considering the sp<sup>3</sup> fraction of the ta-C film. In contrast, there is a large spread in the electronic properties of the ta-C films measured by various groups. Conductive ( $\sim 4$   $\Omega$  cm<sup>-1</sup>) low band gap ( $\sim 0$  eV) [9] as well as resistive ( $10^{-7}$  to  $10^{-11}$   $\Omega$  cm<sup>-1</sup>) high band gap ( $E_{04}$  up to 3 eV)

\*Corresponding author. Tel.: +44-1223-765242; fax: +44-1223-332662.

E-mail address: acf26@eng.cam.ac.uk (A.C. Ferrari).

[10–13] ta-C films have been reported, but with essentially the same  $sp^3$  content. Indeed, unlike the density or Young's modulus which reached 70% or more of the corresponding property in diamond, the reported optical gaps lie between  $\sim 40$  and 55% of the diamond band gap [4,5,12–14], the typical Tauc gap being  $\sim 2.1$ – $2.4$  eV.

The electronic properties of ta-C mainly depend on the local configuration of the  $sp^2$  sites rather than simply the  $sp^3/sp^2$  fraction. Conductive low band gap high  $sp^3$  ta-C films can be formed by annealing resistive high band gap as-deposited ta-C films [12,13,15]. Theoretically, it has been shown that if the  $sp^2$  sites form graphitic clusters in amorphous carbon, the band gap will be significantly reduced [1–3]. However, the formation of large clusters in ta-C is opposed by disorder due to the deposition process [16], and molecular dynamics simulations indicate that the  $sp^2$  sites are unlikely to form large clusters in ta-C [17–19]. The presence of graphitic inclusions from the deposition process, as well as cross-sectional non-uniformity, can reduce the effective gap of the material [20].

Here we report on the deposition of ta-C films with an  $E_{04}$  gap up to 3.5 eV and Tauc gap up to 3.0 eV. This is the highest optical gap ta-C reported in literature measured directly using photothermal deflection spectroscopy (PDS) and UV-Vis spectrophotometry. Although the films exhibit a large optical gap, a large number of defect states was found to fill the mid-gap region. Annealing the samples at 500 °C reduced the defect density and increased the optical gap. This annealing does not significantly change the  $sp^3$  fraction, but gives a 2–3 order of magnitude increase of the conductivity and a significant reduction of the stress [12,13]. This, in principle, shows that it is possible to improve the electronic properties of ta-C.

## 2. Experiment

The ta-C films were deposited using a filtered cathodic vacuum arc system with an integrated off plane double bend (S-bend) magnetic filter. Ta-C films with particle area coverage of less than 0.01% and uniform cross-section were consistently deposited using this system [7,20]. The deposition rate is 5 Å/s and the thickness variation over a 60×60 mm substrate is typically 7% in total. The deposition chamber was evacuated to  $1 \times 10^{-8}$  torr using a turbo molecular pump. From EELS, the  $sp^3$  fraction of the films was  $\sim 88\%$  [7] and the plasmon energy was  $\sim 31.4$  eV.

For the optical gap experiments, ta-C films of 30-nm thickness were deposited on spectral-grade quartz and polished silicon substrates. Independent UV-VIS spectrophotometry measurements, performed on two different systems, and photothermal deflection spectroscopy (PDS) measurements were used to probe the optical

absorption of our samples in the 1–6 eV photon energy range. The calibration of the PDS measurements was performed both by using the same PDS apparatus operating at saturation conditions and by comparison with the optical measurements.

Kramers–Kronig analysis of the low loss EELS spectrum [21] was also performed on free-standing ta-C films prepared by etching the silicon substrates in HF:HNO<sub>3</sub> solution. Momentum resolved EELS measurements were taken at off-axis configuration in order to reduce the contribution of surface losses. The EELS measurement were carried out on a VG 501 scanning transmission electron microscope equipped with a dedicated spectrometer and a McMullan parallel EELS detection system. The energy dependence of the real and imaginary parts ( $\epsilon_1$  and  $\epsilon_2$ ) of the dielectric function were calculated, together with other optical quantities such as the absorption coefficient and the reflectivity [21]. Although a typical energy loss spectrum has a poorer energy resolution than spectrophotometry and gives less reliable data for very low energies due to difficulties in suppressing the zero loss, its energy range is greater [21] and hence provides a better definition of the Tauc gap.

A combination of Raman spectroscopy and electron spin resonance (ESR) was used to further determine the nature of the  $sp^2$  network. The Raman spectra of the ta-C film on silicon substrate were obtained using excitation at 514.5 and 229 nm. The spin density was measured for films deposited on a quartz substrate. The spin density was calibrated by a water diluted TEMPO standard in a capillary tube. The deconvolution of the overall signal into the two contributions was obtained by standard numerical routines.

Temperature-dependent ESR measurements were performed using free-standing ta-C films obtained by etching the silicon substrates. The etching process is the same used to prepare the EELS specimens [10]. Although this is a lengthy procedure, it avoids any inclusion of particles, which occurs if the powder was prepared by performing a very long deposition in order to let the sample delaminate [22]. Measurements on the free-standing films, kept in a quartz tube under static vacuum, were first performed at room temperature in order to verify the results obtained for the quartz deposited specimen.

Finally, one set of as-deposited samples was annealed to 500 °C under vacuum conditions. This temperature was specifically chosen as it is low enough not to change the  $sp^3$  content, but high enough to influence the configuration of the  $sp^2$  phase [12,13]. The optical absorption and ESR measurements as described above were thus repeated on these samples.

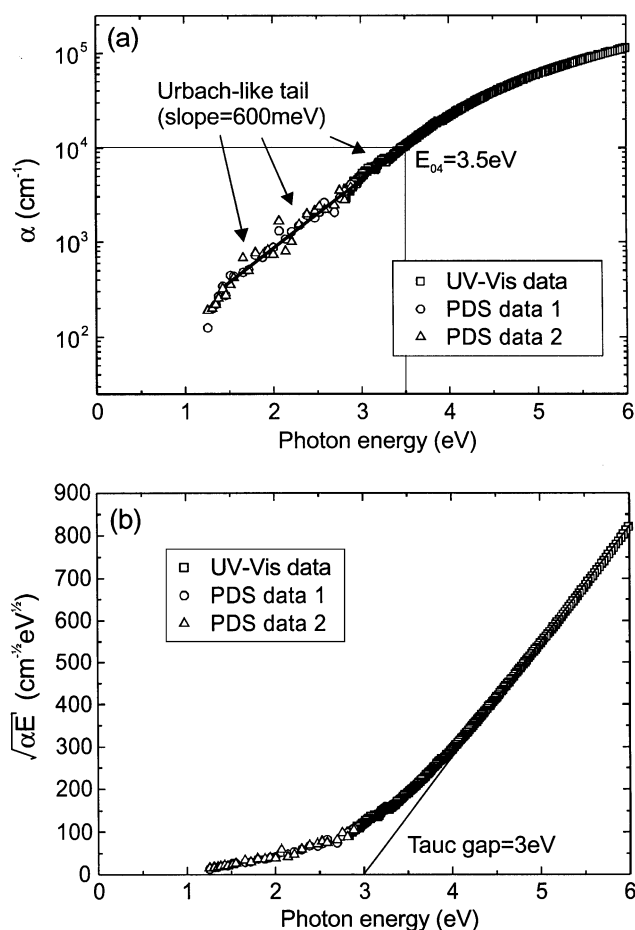


Fig. 1. (a) Absorption coefficient,  $\alpha$ , vs. photon energy and (b) Tauc plot for the high gap ta-C film derived from a combination of PDS and UV-Vis measurements. The  $E_{04}$  gap is  $\sim 3.5$  eV and the Tauc gap (fitted from 4 to 6 eV) is  $\sim 3$  eV. An Urbach-like trend, is found at low energies.

### 3. Results and discussion

The optical absorption characteristics of the as-deposited ta-C films are plotted in Fig. 1. Good agreement was found between the measurements and it was possible to combine the PDS and UV-Vis data to provide a complete picture of the absorption coefficient from 1 to 6 eV. The  $E_{04}$  gap, defined as the energy at which the absorption coefficient  $\alpha = 10^4 \text{ cm}^{-1}$ , was  $\sim 3.5$  eV. The Tauc gap, extracted from the Tauc plot of Fig. 1b, was  $\sim 3.0$  eV. This result was consistently reproduced on measurements made on a series of different samples deposited under the same conditions. The results of the Kramers–Kronig analysis of EELS data are shown in Fig. 2a,b. Fig. 2a plots  $\epsilon_1$  and  $\epsilon_2$ . Fig. 2b shows, over a wider energy range, that the Tauc gap was  $\sim 3.5$  eV.

Despite the large optical gap, Figs. 1a,b show that the band tail only slowly decreases inside the gap and the absorption coefficient exhibits an exponential decay from 4 eV down to 1 eV. The Urbach slope was

determined to be  $\sim 600$  meV, which is higher than what is usually found in ta-C [15]. Thus, these high optical ta-C films contained a high density of tail states.

Fig. 3 shows the comparison between the 514.5 nm and 229 nm Raman spectra of the ta-C film. No D peak was present and the dispersion of the G peak position between visible and UV Raman was  $\sim 130 \text{ cm}^{-1}$ , the highest amongst amorphous carbons [23,24], thus confirming that aromatic clusters are absent in the matrix. The very high G position in the UV Raman spectrum can only be due to short C=C  $\text{sp}^2$  chains, if one considers that the C=C stretching vibration in ethylene is  $\sim 1630 \text{ cm}^{-1}$ .

The measured spin density of our films was  $7.5 (\pm 2.5) \times 10^{20} \text{ spins/cm}^3$ , which is amongst the highest values reported for ta-C [4,15]. In theoretical calculations of the electronic density of states of ta-C [25], electronic defect states were found to dominate at the Fermi level. These are due to isolated  $\text{sp}^2$  units,  $\text{sp}^2$  pairs with strong dihedral distortions, and non-bonding  $\pi$  states; all these contribute to the ESR signal. The comparison of the signals linewidths recorded from 4 to 300 K is shown in Fig. 4. A line-width decrease with increasing temperature can be observed. This is *opposite* to the behaviour reported [22] previously for a ta-C sample, obtained by using powders collected over a

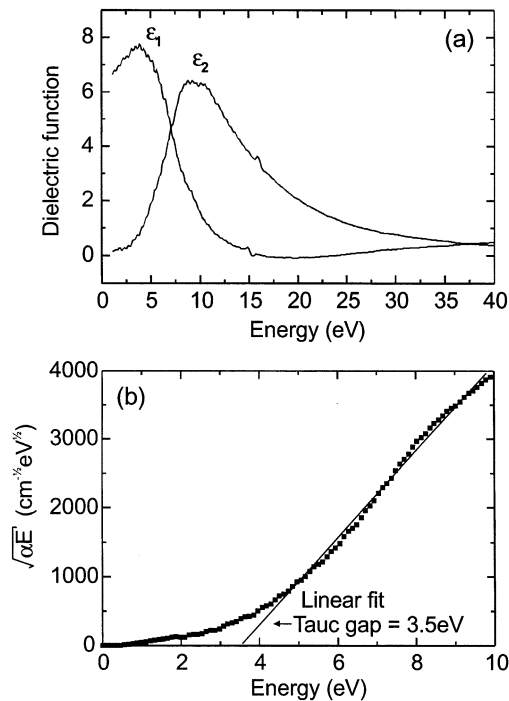


Fig. 2. (a) Real and imaginary part ( $\epsilon_1$  and  $\epsilon_2$ ) of the dielectric function of a high gap ta-C film derived from a Kramers–Kronig analysis of the low loss EELS spectrum. (b) Tauc plot from absorption data derived by EELS. The Tauc gap is  $\sim 3.5$  eV when fitted over the wider energy range from 4 to 10 eV, which confirms the optical data in Fig. 1.

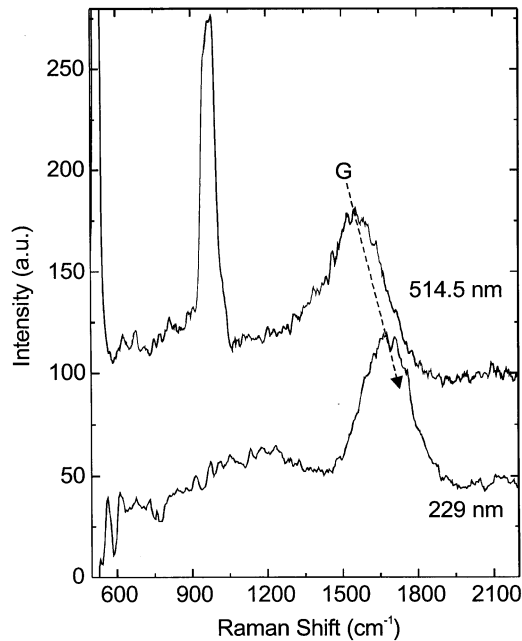


Fig. 3. The 514.5 and 229 nm Raman spectra of a high gap ta-C film. Unpolarised Raman spectra were acquired in backscattering geometry. A Renishaw micro-Raman system modified for UV excitation was used to record the spectrum at 229 nm. Another Renishaw system was used for 514.5 nm. No D peak is present. The dispersion of the G peak position between visible and UV Raman is  $\sim 130 \text{ cm}^{-1}$ .

long deposition time from a single bend FCVA. The line-width is determined mainly by the spin–spin relaxation time [26]. The spin–spin interaction is an exchange coupling, which does not dissipate energy. The energy is dissipated by interactions with the lattice. If the motion occurs by hopping from one site to the other, a decrease of line-width with temperature is expected, since the line-width is proportional to the inverse of the mobility [27] and the mobility is thermally activated. Thus, the mobility of carriers is thermally activated for our samples and electrical conduction occurs by hopping, while it was previously reported [22] as being due to extended or overlapping states (i.e. percolating through the sample). The new result is consistent with that expected for such high optical gap films. The previous results [22] may be due to the presence of graphite particles which were generated from the less well filtered deposition process carried over long deposition times, and the presence of layers of different density and higher  $\text{sp}^2$  clustering which are usually present in these previous film [7].

The challenge now is to reduce the number of defects, whilst maintaining or even further widening the optical gap. This could be achieved by increasing the delocalisation of the  $\text{sp}^2$  phase, but without increasing the  $\text{sp}^2$  content. This concept was demonstrated by annealing the as-deposited samples at  $500^\circ\text{C}$  in vacuum. Fig. 5 plots the optical absorption coefficient of the annealed

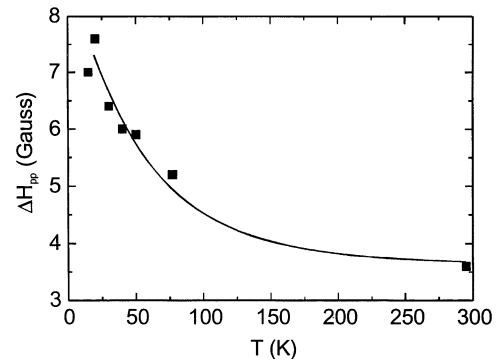


Fig. 4. Temperature dependence of the peak-to-peak line-width as obtained by fitting the ESR spectra with Lorentzian shapes. The continuous line represents a guide for the eye. A trend of decrease in line-width with increasing temperature can be observed, which is opposite to previous measurements [22].

ta-C film with the previous low gap ta-C film for comparison.

In a semi-logarithmic scale, we note that the absorption for previous low gap ta-C films have a parabolic decay from 3 to 1 eV. However, the low energy absorption trend of our as-deposited high gap ta-C films was exponential and Urbach-like (Fig. 1a). After annealing, the low energy absorption trend of the high gap ta-C film reverted to the parabolic-like decay similar to the low gap ta-C film. There was also a slight increase of 0.1 eV in the  $E_{04}$  of annealed high gap ta-C film, which was consistently detected for other annealed samples.

The parabolic optical absorption spectra in the low energy regime has been attributed [28–30] to  $\pi$ – $\pi^*$  transitions between Gaussian-shaped distributions of

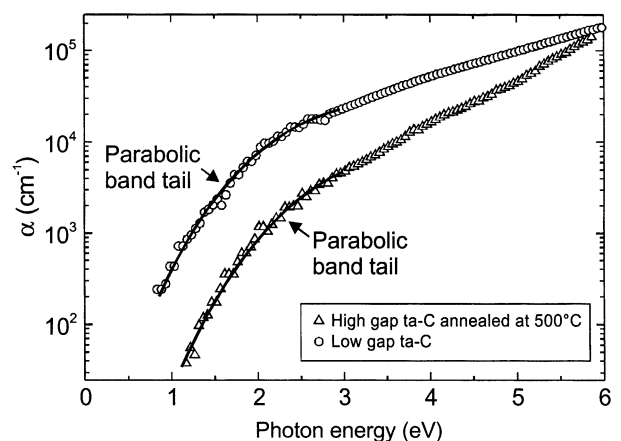


Fig. 5. Absorption coefficient,  $\alpha$ , vs. photon energy plot for a low gap ta-C film and an annealed high gap ta-C film. Both films exhibit parabolic decay in the absorption coefficient at low energies, which arise from  $\pi$ – $\pi^*$  transitions. After annealing, the high gap film has lower absorption at low energies because of the parabolic decay compared with the Urbach-like decay of Fig. 1. This implies that less tail states are present after annealing.

localised  $\pi$  and  $\pi^*$  states 1–3 eV above and below the local atomic energy level. These transitions typically exist in low gap ta-C and a-C:H films which thus exhibit a parabolic decay in a semi-log plot of their absorption coefficient for low photon energies.

In contrast, exponential optical absorption spectra could be connected to transitions involving localised, exponential tails of  $\sigma$ -states. Thus, in the highly disordered as-deposited high gap ta-C film [ $N_s = 7.5(\pm 2) \times 10^{20} \text{ cm}^{-3}$ ], the transitions from the band-tails of  $\sigma$ -states dominate to give the exponential decay of the absorption coefficient at low energies.

After annealing the high gap ta-C film, the band-tails of  $\sigma$ -states have less participation in the low energy optical transitions and more  $\pi$ – $\pi^*$  transitions must be occurring instead in order to give rise to the parabolic shape in the absorption spectra. We thus attribute the increase in  $\pi$ – $\pi^*$  transitions to more aligned  $sp^2$  pairs (or chains) appearing in the film. ESR measurements on the annealed ta-C show that the spin density has been reduced by a factor of 3 to  $N_s = 2.5(\pm 2) \times 10^{20} \text{ cm}^{-3}$ . This confirms that less disorder is present after annealing. Moreover, temperature-dependent ESR measurements also showed an order of magnitude increase in the delocalisation of the spin carriers in the annealed sample compared with the as-deposited sample [31].

#### 4. Conclusions

Using the S-bend FCVA, we succeeded in depositing very high optical gap ta-C films, with  $E_{04}$  values of  $\sim 70\%$  of the minimum (indirect) band gap of diamond and more than 1 eV in excess of the usually reported optical gap of ta-C films. This high gap has been confirmed by PDS, UV-Vis and EELS measurements. These films are free of graphitic inclusions and have an extremely uniform cross-section, in contrast to lower gap ta-C samples [7,20]. The observed gap of  $\sim 3.5$  eV is close to the calculated limit for ta-C of high  $sp^3$  content [5,25]. This high optical gap material, however, exhibits a high defect density. The defects are from band-tails of  $\sigma$ -states which give rise to an Urbach-like absorption decay from 1 to 4 eV. For ta-C to be suitable as an electronic material, the defects must be removed whilst maintaining the high gap. This was demonstrated by annealing the film under conditions which we previously found to increase its conductivity and retain its  $sp^3$  content [12,13]. The defect density was decreased, dihedral alignment of the  $\pi$  states increased and the optical gap was maintained.

#### Acknowledgments

K.B.K.T. acknowledges the support of the Association of Commonwealth Universities and the British Council.

A.C.F. acknowledges funding from an E.U. Marie Curie fellowship.

#### References

- [1] J. Robertson, *Prog. Solid State Chem.* 21 (1991) 199.
- [2] J. Robertson, *Pure Appl. Chem.* 66 (1994) 1789.
- [3] J. Robertson, *Adv. Phys.* 35 (1986) 317.
- [4] D.R. McKenzie, *Rep. Prog. Phys.* 59 (1996) 1611.
- [5] Y. Lifshitz, *Diamond Relat. Mater.* 8 (1999) 1659.
- [6] A.A. Voevodin, M.S. Donley, *Surf. Coat. Technol.* 82 (1996) 199.
- [7] A.C. Ferrari, A. Libassi, B.K. Tanner, et al., *Phys. Rev. B* 62 (2000) 11089.
- [8] A.C. Ferrari, J. Robertson, M.G. Beghi, C.E. Bottani, R. Ferulano, R. Pastorelli, *Appl. Phys. Lett.* 75 (1999) 1893.
- [9] J. Schwan, S. Ulrich, H. Roth, et al., *J. Appl. Phys.* 79 (1996) 1417.
- [10] P.J. Fallon, V.S. Veerasamy, C.A. Davis, et al., *Phys. Rev. B* 48 (1993) 4777.
- [11] S. Xu, B.K. Tay, H.S. Tan, et al., *J. Appl. Phys.* 79 (1996) 7234.
- [12] A.C. Ferrari, B. Kleinsorge, N.A. Morrison, A. Hart, V. Stolojan, J. Robertson, *J. Appl. Phys.* 85 (1999) 7191.
- [13] J.P. Sullivan, T.A. Friedmann, A.G. Baca, *J. Electron. Mater.* 26 (1997) 1021.
- [14] M. Chhowalla, J. Robertson, C.W. Chen, et al., *J. Appl. Phys.* 81 (1997) 139.
- [15] B. Kleinsorge, A.C. Ferrari, J. Robertson, W.I. Milne, *J. Appl. Phys.* 88 (2000) 1149.
- [16] J. Robertson, *Diamond Relat. Mater.* 4 (1995) 297.
- [17] D.A. Drabold, P.A. Fedders, P. Strumm, *Phys. Rev. B* 49 (1994) 16415.
- [18] T. Frauenheim, P. Blaudeck, U. Stephan, G. Jungnickel, *Phys. Rev. B* 50 (1994) 6709.
- [19] N.A. Marks, D.R. McKenzie, B.A. Paulthorpe, M. Bernasconi, M. Parrinello, *Phys. Rev. B* 54 (1996) 9603.
- [20] K.B.K. Teo, S.E. Rodil, J.T.H. Tsai, A.C. Ferrari, J. Robertson, W.I. Milne, *J. Appl. Phys.* 89 (2001) 3706.
- [21] R.F. Egerton, *Electron Energy Loss Spectroscopy in the Electron Microscope*, Plenum, New York, 1986.
- [22] G. Fusco, A. Tagliaferro, W.I. Milne, J. Robertson, *Diamond Relat. Mater.* 6 (1997) 783.
- [23] A.C. Ferrari, J. Robertson, *Phys. Rev. B* 61 (2000) 14095.
- [24] A.C. Ferrari, J. Robertson, *Phys. Rev. B* 64 (2001) 075414.
- [25] G. Jungnickel, T. Kohler, T. Frauenheim, M. Haase, P. Baudeck, U. Stephan, *Diamond Relat. Mater.* 5 (1996) 175.
- [26] J.E. Wertz, J.R. Bolton, *Electron Spin Resonance*, Chapman and Hall, London, 1972.
- [27] H. Dersch, J. Stuke, J. Beichler, *Phys. Status Solidi B* 107 (1981) 307.
- [28] D. Dasgupta, F. Demichelis, C.F. Pirri, A. Tagliaferro, *Phys. Rev. B* 43 (1991) 2131.
- [29] A. Zeinert, H.J. von Bardeleben, R. Bouzerar, *Diamond Relat. Mater.* 9 (2000) 728.
- [30] M.L. Theye, V. Paret, A. Sadki, *Diamond Relat. Mater.* 10 (2001) 182.
- [31] G. Fanchini, A. Tagliaferro, D. Dasgupta et al., *J. Non-Cryst. Solids*, to be published (2002).